Electrostatic Solar Sail: A Propellantless Propulsion Concept for an Interstellar Probe Mission

Anthony M DeStefano[1] (anthony.m.destefano@nasa.gov), Bruce M Wiegmann[2] , Mike Bangham[3] , Thomas Bryan[1] , John Carr[1] , Andrew Heaton[1] , Les Johnson[1] , Daniel Tyler[1] , Kenneth H Wright Jr[4] and Nobie Stone[2]

(1)NASA Marshall Space Flight Center, Huntsville, AL, United States, (2)Retired, Huntsville, AL, United States, (3)Bangham Engineering Incorporated, Huntsville, United States, (4)Universities Space Research Association, Huntsville, AL, United States

1: Introduction

The propulsion of an electrostatic solar sail (E-Sail) is obtained by extracting momentum from the solar wind through electrostatic repulsion of the positively charged solar wind ions (see Figure 1). The positively charged solar wind protons are deflected by the electric field created around the tethers. This electric field grows in diameter as the spacecraft moves away from the Sun, therefore the E-Sail effective area grows. The growth of the E-Sail effective area allows the propulsive force to decrease as 1/r up to distances of 20 AU as it moves away from the Sun, unlike solar sail propulsion whose thrust decreases as $1/r^2$ but only to distances of 5 AU. This propulsive force is created without using propellant and, therefore, E-sail avoids both the mass and complexity of chemical rockets (that require large amounts of propellant, propellant storage tanks, plumbing, valves, and insulation).

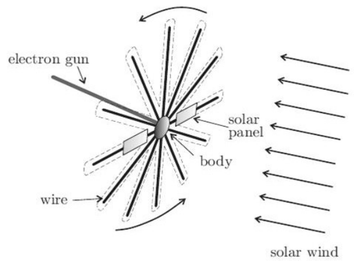

Figure 1: Notional Electrostatic sail Propulsion System.

2: Analytical Thrust Model

The **force per unit length, f,** of an ion beam incident on a single positively charged tether depends on the ion beam properties as well as the tether potential bias. Assuming normal incidence and singly charged ions, the minimum required variables are:

- Ion density (n_0) and speed (V_0)
- Electron density (n_e) and temperature (T_e)
- Tether radius (r_w) and potential bias (ϕ_0)

The potential bias of the tether creates a barrier that extends several Debye lengths (λ_D), called the **proton deflection sheath, r_s** (see Figure 2). If we assume the ions bounce off the barrier specularly, the force per unit length can be solved analytically, given by

$$f = 2.66 n_0 m_0 V_0^2 r_s. \qquad \text{(Eq. 1)}$$

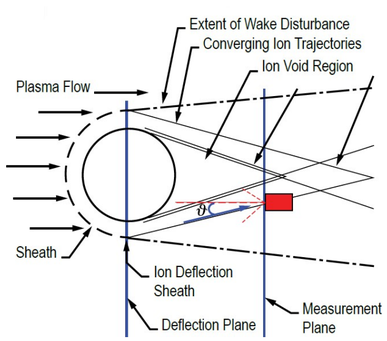

Figure 2: An illustration showing the regions of disturbed plasma flow. The proton deflection sheath is the distance from the wire to the extent of the wake disturbance.

Conceptually, we expect the proton deflection sheath to increase as we increase the potential bias of the wire since the effective barrier cross-section is increased. To effectively repel the incoming ions, the tether potential bias should be greater than the ion kinetic energy.

3: Link to Laboratory Data

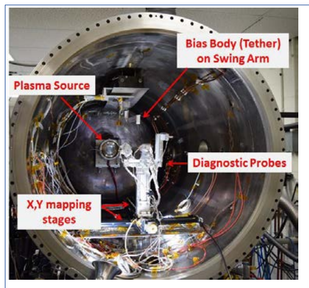

End view of vacuum test chamber.

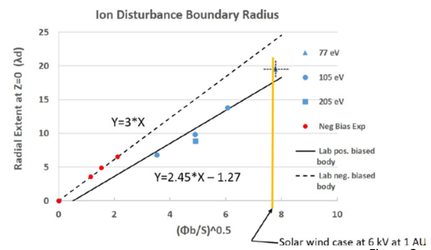

Figure 4: Radial extent of ion disturbance boundary versus normalized body potential and Mach number. The error bars drawn on the 77 eV point are the same for the other blue symbols.

Figure 3:

In the analytic thrust model shown in Eq. 1, the proton deflection sheath r_s must be solved in terms of ion beam and tether properties. The lab results are casted into dimensionless parameters $\boldsymbol{\Phi_0 = \frac{q_e \phi_0}{k_B T_e}}$, the **normalized tether potential**, and $\boldsymbol{S = \sqrt{\frac{m_p V_0^2}{2 k_B T_e}}}$, the **Mach number**, so we can define the proton deflection sheath in terms of the lab measurements. The 1 AU solar wind case in terms of the dimensionless parameters is shown by the *yellow* line in Figure 4, where the 77 eV lab case achieves the same parametric ratio. These lab measurements are summarized in Figure 4 by the *blue* markers for ion (Ar^+) energies of 77 eV, 105 eV, and 205 eV.

Assuming r_s is proportional to $\sqrt{\frac{\Phi_0}{S}}$, we make a linear fit given by

$$r_s = \alpha \lambda_D \sqrt{\frac{\Phi_0}{S}}, \qquad \text{(Eq. 2)}$$

where $\boldsymbol{\alpha = 2.45}$ derived from lab data, as shown in Figure 4. In reality, once the ion kinetic energy is near or exceeds the wire potential energy, the proton deflection sheath stops growing, as shown in Figure 6.

4: Numerical Thrust Model

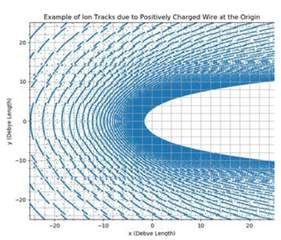

Figure 5: Example of ion particle tracks exposed to a positively charged wire.

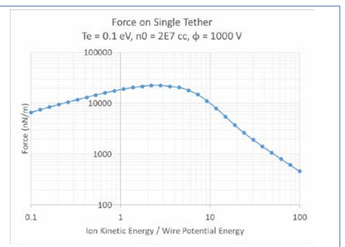

Figure 6: Example of the force as a function of the ion-wire energy ratio.

We have developed a **test particle model** that tracks particle trajectories (see Figure 5) and computes the net force per unit length on a positively charged infinite wire (see Figure 6). The potential field we employ assumes implicitly the full plasma (electrons and ions), given by (see Eq. 2 of Janhunen & Sandroos 2007)

$$\phi(r) = \phi_0 \ln\left[1 + \frac{r_0^2}{r^2}\right] \ln\left[1 + \frac{r_0^2}{r_w^2}\right], \qquad \text{(Eq. 3)}$$

where r_0 is twice the Debye length and r_w is the wire radius.

5: Thrust Dependence on Solar Distance

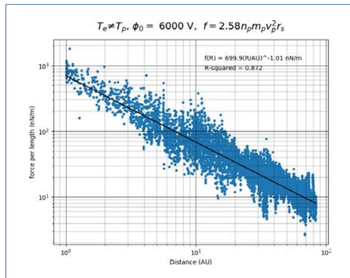

Figure 7: Force vs distance from the Sun using Voyager Eq. 1 showing the 1/r force relation.

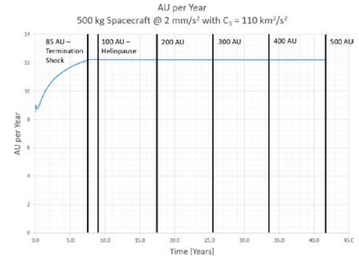

Figure 8: AU per year vs travel time assuming a data in characteristic acceleration of 2 mm/s².

We derive the force as a function of solar distance by plugging in Voyager plasma data into Eq. 1, where we fit a power-law relation showing a slope of -1.01, as shown in Figure 7. By brief analysis of Eq. 1, since the density n_0 falls as $1/r^2$ and the proton deflection sheath r_s grows as r, we expect the force to fall as 1/r.

Taking this 1/r relation, we did a basic spacecraft trajectory analysis in Copernicus to show the concept that an E-sail with a characteristic acceleration (CA) of 2 mm/s² at 1 AU and a C_3 of 110 km²/s² (SLS Block 1b) can reach the heliopause within 10 years, see Figure 8. To achieve a CA of 2 mm/s² any combination of longer tethers, a greater number of tethers, or a higher wire potential would be needed to increase the net thrust.

6: Conclusion and Forward Work

Since the force as a function of solar distance drops as 1/r for an E-sail, this propellentless propulsion system is able to accelerate at greater solar distances as compared to solar sail technology. In addition, the E-sail takes advantage of the solar wind plasma in order to propel itself using a series of positively charged tethers. This allows for quick travel times to the heliopause and beyond, without complex Oberth maneuvers or gravity assists.

For forward work, we plan to make measurements of the force of an ion beam on a positively charged tether in a vacuum chamber in order to test the various thrust models that have been proposed in the literature. Other questions about the E-sail technology we aim to tackle are tether deployment, spin up of the E-sail tethers, attitude control, and orbital maneuvers such as plane changes.

7: Acknowledgements

We would like to acknowledge support from award 14-NIAC14B-0075 (NIAC phase I and II) and the MSFC FY20 CIF titled, “Direct Thrust Measurements of Electrostatic Sail Tethers.”

8: References

Janhunen, P. and Sandroos, A., 2007, March. Simulation study of solar wind push on a charged wire: basis of solar wind electric sail propulsion. In Annales Geophysicae (Vol. 25, No. 3, pp. 755-767).

SH51E-3319
AGU Dec. 9-13, 2019